Bioorganometallic Chemistry

DOI: 10.1002/anie.201000097

Label-Free Imaging of Metal–Carbonyl Complexes in Live Cells by Raman Microspectroscopy**

Konrad Meister, Johanna Niesel, Ulrich Schatzschneider, Nils Metzler-Nolte,* Diedrich A. Schmidt, and Martina Havenith**

The search for novel metal complexes with therapeutic activity, in particular against cancer and infectious diseases, is an active and important area of research in medicinal inorganic chemistry. In addition to the well-studied platinum- and ruthenium-based coordination complexes, organometallic compounds have gained considerable importance in recent years.[1–4] Of those, metal–carbonyl compounds are steadily increasing in interest, with some exhibiting remarkable antitumor activity.[5,6] The most prominent example is probably the use of such compounds as "solid storage forms" for carbon monoxide. These CO-releasing molecules (CORMs) allow the biological action of this important small molecule messenger to be investigated.[7–12]

To elucidate the biological mode of action of any drug candidate it is mandatory to obtain a detailed picture of the intracellular distribution of such substances and how it evolves over time. Until now, the localization of metal complexes inside cells has been studied using X-ray fluorescence (XRF)[13,14] and atomic absorption spectroscopy (AAS).[15] While AAS offers high sensitivity but almost no spatial resolution, XRF requires intense X-ray sources such as synchrotrons which will cause damage to biological tissue and is also not routinely available as an analytical technique.

Most cellular studies therefore use fluorescence microscopy.[16] Furthermore, this technique requires the additional attachment of a fluorescent label, which might be difficult. Optical excitation can also cause additional problems such as the onset of photochemical reactions or photobleaching. Moreover, the label can alter the biodistribution and properties of the molecule of interest, as recently shown for ruthenium–bipyridyl complexes.[17]

Efforts have been made to overcome these limitations by identifying biologically active metal complexes which show inherent fluorescence in vivo, but this has only been possible for a small number of metal–ligand combinations. Thus, it is highly desirable to develop innovative and generally applicable imaging techniques for the study of the uptake and distribution of bioactive metal complexes which do not require any labeling or special photophysical properties but instead use the intrinsic spectroscopic signature of the compound of interest.

Raman microspectroscopy is emerging as a powerful non-invasive method to assess and image cellular compartments and processes without further sample preparation or labeling. Since Puppels et al. first showed the feasibility of confocal Raman microspectroscopy for imaging cells,[18] its ability to study whole cells and subcellular organelles such as the nucleus and chromatin,[19] mitochondria,[20] and lipid bodies[21] has been demonstrated by various research groups. Apart from imaging subcellular features, Raman imaging has been used to follow the uptake of molecules by cells.[22,23] So far, however, these investigations have been restricted to the incorporation of deuterated building blocks as sensitive and specific markers into bio(macro)molecules.

Herein, we investigate the uptake and cellular distribution of the new manganese-based CORM $[Mn(tpm)(CO)_3]Cl$ (tpm = tris(1-pyrazolyl)methane), which has photoinduceable cytotoxic activity against cancer cells.[11] Metal–carbonyl complexes such as $[Mn(tpm)(CO)_3]Cl$ show strong C≡O stretching vibrations between 1800 and 2200 cm^{-1}, a region where vibrational signals from the constituents of the cell are negligible. We show that the C≡O vibrations of this compound can be used as an ideal marker for imaging these complexes in living cancer cells.

Although the spectroscopic signature of metal–carbonyl compounds has already been used in bioanalytical techniques such as the carbonyl–metal immunoassay (CMIA),[24] their use in cellular imaging is so far unprecedented, except for an investigation of osmium–carbonyl clusters in dried cells by using infrared microscopy.[25]

The IR and Raman spectra of solid $[Mn(tpm)(CO)_3]Cl$ show strong C≡O stretching vibrations at about 1944 and 2050 cm^{-1}, as expected for local C_{3v} symmetry (Figures S1 and S2 A in the Supporting Information). The different relative intensities of the two peaks can be explained by the distinct selection rules for Raman and IR spectroscopy. The O–H stretching vibration localized at about 3400 cm^{-1} dominates the spectrum of a 2 mM aqueous solution of [Mn(tpm)-

[*] K. Meister, Dr. D. A. Schmidt, Prof. Dr. M. Havenith
Lehrstuhl für Physikalische Chemie II, Ruhr-Universität Bochum
Universitätsstrasse 150, 44801 Bochum (Germany)
E-mail: martina.havenith@rub.de
Homepage: www.rub.de/pc2
J. Niesel, Dr. U. Schatzschneider, Prof. Dr. N. Metzler-Nolte
Lehrstuhl für Anorganische Chemie I, Ruhr-Universität Bochum
Universitätsstrasse 150, 44801 Bochum (Germany)
E-mail: ulrich.schatzschneider@rub.de
nils.metzler-nolte@rub.de
Homepage: www.rub.de/ac1

[**] This work was supported by the DFG within the "Biological function of organometallic compounds" (FOR 630) and the Research Department "Interfacial Systems Chemistry" at the RUB. We acknowledge financial support for the Raman microscope under grant BMBF 05KS7PC2. J.N. thanks the RUB Research School for a PhD fellowship. We thank E. Bründermann and A. Halang for help with handling of the Raman spectrometer and cell culture.

Supporting information for this article is available on the WWW under http://dx.doi.org/10.1002/anie.201000097.

$(CO)_3$]Cl, but one C≡O stretching band can still be identified unambiguously (see Figure S2B in the Supporting Information). The main C≡O band shifts from 1944 to 1963 cm^{-1} in an aqueous environment. Additional peaks from the metal–carbonyl complex appear in the region between 600 and 1800 cm^{-1}, but these bands show a strong overlap with the signals of other cellular constituents.

Figure 1 A shows an optical image of a HT29 cell incubated for 3 h with a 2 mM aqueous solution of [Mn(tpm)$(CO)_3$]Cl. The cell shows a characteristic size of about

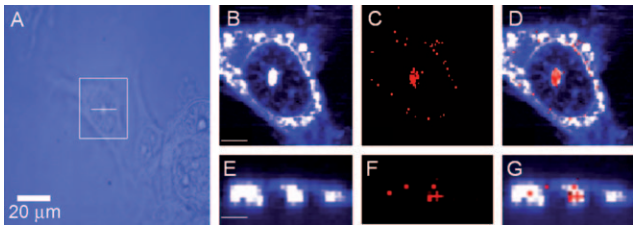

Figure 1. A) Optical image of a HT29 human colon cancer cell incubated with an aqueous solution (2 mM) of [Mn(tpm)$(CO)_3$]Cl for 3 h. B, C) Raman images reconstructed from integrating the intensities of the C–H and C≡O stretching peaks. The integration range was 2800–3050(±2) cm^{-1} for (B) and 1945–1965(±2) cm^{-1} for (C). D) Overlaid image of panels (B) and (C). E–G) Cross-section Raman images along the *x*,*z*-direction of the same cell. Scanning positions are indicated by the white bar in the optical image. The scale bar for the Raman images is 6 μm.

30 μm × 30 μm. The Raman image of the same cell reconstructed from the C–H stretching vibration at 2800 to 3050 cm^{-1} is shown in Figure 1 B. The general shape of the cell as well as the nucleus, nuclear membrane, and the surrounding cytoplasm can clearly be seen. Figure 1 C shows the reconstructed image of the maximum integrated intensities of the C≡O stretching vibration. A distinct circular pattern with further accumulation in the center of the nucleus can be seen. Figure 1 D shows an overlay of Figure 1 B and C. After incubation for 3 h, the compound has clearly become associated with the cell, predominantly with the nucleus and the nuclear membrane. To prove that the compound is indeed internalized in the cell and not just adsorbed on the outer cell surface, a cross-section along the *x*,*z* direction was recorded (Figure 1 E–G). These images clearly prove that the compound has penetrated the cellular membrane and is localized mainly in the nuclear membrane and the nucleolus.

Figure 2 A shows an averaged Raman spectrum of the cell in a region where the carbonyl bands of the [Mn(tpm)$(CO)_3$]Cl inside the cell have their maximum intensity. A typical averaged spectrum from within the cytoplasm where almost no [Mn(tpm)$(CO)_3$]Cl is located is also shown. The bands arising from the different cell constituents are clearly visible in both cases. Dominant features can be attributed to the C–H stretching vibrations at 2900 cm^{-1}, the amide I band at 1655 cm^{-1}, the C–H and CH_2 bending deformations at 1450 cm^{-1}, as well as the ring-breathing mode of phenylalanine at 1002 cm^{-1}. A significant difference between the two spectra is seen in the range between 1900 and 2100 cm^{-1}. A peak at 1963 cm^{-1} is clearly visible in

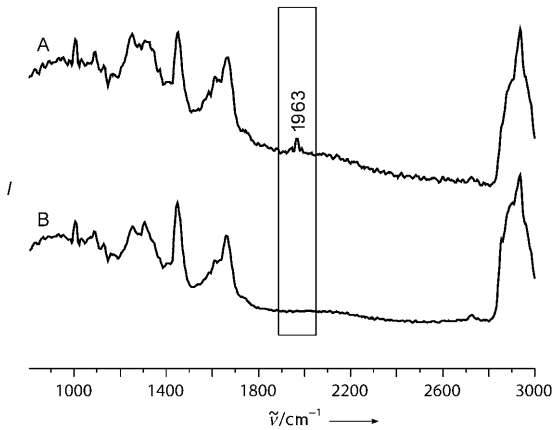

Figure 2. A) Averaged Raman spectrum of the maximum [Mn(tpm)$(CO)_3$]Cl signal inside a HT29 human colon cancer cell and B) a typical averaged Raman spectrum from a region within the cell lacking any metal complex.

Figure 2 A which can be unambiguously assigned to the C≡O stretching vibration of [Mn(tpm)$(CO)_3$]Cl which has penetrated inside the cell. This signal is absent in Figure 2 B, which was recorded in a region of the cell lacking any metal complexes.

The 3D Raman imaging of a stable, water-soluble organometallic carbonyl complex in living cancer cells has been reported here for the first time, and utilized to study its uptake and intracellular fate. The C≡O stretching vibrations of [Mn(tpm)$(CO)_3$]Cl serve as intrinsic labels, thereby making a label-free identification and localization of this metal complex inside living cells possible. Such organometallic compounds as well as their biochemical and cytotoxic properties are of fundamental interest in the fields of medicinal chemistry and antitumor chemotherapy. The compound was shown to target the nucleus, with significant accumulation in the nuclear membrane as well as the nucleoli. Given the established photoinduced cytotoxicity of [Mn(tpm)$(CO)_3$]Cl as a CORM, these results provide new insights into the mode of biological action of this class of compounds.

Moreover, Raman microspectroscopy has been shown to be a powerful tool for bioimaging. This study thus introduces metal–carbonyl complexes as a new imaging modality with tailor-made properties. The conjugation of organometallic complexes to biomolecules offers a wide variety of possibilities.[12,26,27] Hence, this study will open the way to new insights into drug uptake mechanisms and intracellular targeting of organometallic drug candidates, as well as for other molecules such as peptides which were tagged with such derivatives.

Received: January 7, 2010
Published online: March 26, 2010

Keywords: bioorganometallic chemistry · infrared microscopy · medicinal chemistry · metal–carbonyl complexes · molecular imaging

[1] G. Jaouen, *Bioorganometallics*, Wiley-VCH, Weinheim, **2006**.
[2] C. G. Hartinger, P. J. Dyson, *Chem. Soc. Rev.* **2009**, *38*, 391 – 401.

[3] M. A. Jakupec, M. Galanski, V. B. Arion, C. G. Hartinger, B. Keppler, *Dalton Trans.* **2008**, 183 – 194.
[4] A. F. A. Peacock, P. J. Sadler, *Chem. Asian J.* **2008**, *3*, 1890 – 1899.
[5] I. Ott, B. Kircher, C. P. Bagowski, D. H. W. Vlecken, E. B. Ott, J. Will, K. Bensdorf, W. S. Sheldrick, R. Gust, *Angew. Chem.* **2009**, *121*, 1180 – 1184; *Angew. Chem. Int. Ed.* **2009**, *48*, 1160 – 1163.
[6] D. Schlawe, A. Majdalani, J. Velcicky, E. Hessler, T. Wieder, A. Prokop, H. G. Schmalz, *Angew. Chem.* **2004**, *116*, 1763 – 1766; *Angew. Chem. Int. Ed.* **2004**, *43*, 1731 – 1734.
[7] T. R. Johnson, B. E. Mann, J. E. Clark, R. Foresti, C. J. Green, R. Motterlini, *Angew. Chem.* **2003**, *115*, 3850 – 3858; *Angew. Chem. Int. Ed.* **2003**, *42*, 3722 – 3729.
[8] R. Motterlini, B. E. Mann, R. Foresti, *Expert Opin. Invest. Drugs* **2005**, *14*, 1305 – 1318.
[9] J. Boczkowski, J. J. Poderoso, R. Motterlini, *Trends Biochem. Sci.* **2006**, *31*, 614 – 621.
[10] B. E. Mann, R. Motterlini, *Chem. Commun.* **2007**, 4197 – 4208.
[11] J. Niesel, A. Pinto, H. W. P. N'Dongo, K. Merz, I. Ott, R. Gust, U. Schatzschneider, *Chem. Commun.* **2008**, 1798 – 1800.
[12] H. Pfeiffer, A. Rojas, J. Niesel, U. Schatzschneider, *Dalton Trans.* **2009**, 4292 – 4298.
[13] J. B. Waern, H. H. Harris, B. Lai, Z. Cai, M. M. Harding, C. T. Dillon, *J. Biol. Inorg. Chem.* **2005**, *10*, 443 – 452.
[14] R. A. Alderden, H. R. Mellor, S. Modok, M. D. Hall, S. R. Sutton, M. G. Newville, R. Callaghan, T. W. Hambley, *J. Am. Chem. Soc.* **2007**, *129*, 13400 – 13401.
[15] S. I. Kirin, I. Ott, R. Gust, W. Mier, T. Weyhermuller, N. Metzler-Nolte, *Angew. Chem.* **2008**, *120*, 969 – 973; *Angew. Chem. Int. Ed.* **2008**, *47*, 955 – 959.
[16] F. Noor, A. Wustholz, R. Kinscherf, N. Metzler-Nolte, *Angew. Chem.* **2005**, *117*, 2481 – 2485; *Angew. Chem. Int. Ed.* **2005**, *44*, 2429 – 2432.
[17] C. A. Puckett, J. K. Barton, *J. Am. Chem. Soc.* **2009**, *131*, 8738 – 8739.
[18] G. J. Puppels, F. F. M. De Mul, C. Otto, J. Greve, M. Robert-Nicoud, D. J. Arndt-Jovin, T. M. Jovin, *Nature* **1990**, *347*, 301 – 303.
[19] N. Uzunbajakava, A. Lenferink, Y. Kraan, E. Volokhina, G. Vrensen, J. Greve, C. Otto, *Biophys. J.* **2003**, *84*, 3968 – 3981.
[20] C. Matthäus, T. Chernenko, J. A. Newmark, C. M. Warner, M. Diem, *Biophys. J.* **2007**, *93*, 668 – 673.
[21] C. Krafft, T. Knetschke, R. H. W. Funk, R. Salzer, *Vib. Spectrosc.* **2005**, *38*, 85 – 93.
[22] C. Matthäus, A. Kale, T. Chernenko, V. Torchilin, M. Diem, *Mol. Pharm.* **2008**, *5*, 287 – 293.
[23] H. J. van Manen, Y. M. Kraan, D. Roos, C. Otto, *Proc. Natl. Acad. Sci. USA* **2005**, *102*, 10159 – 10164.
[24] A. Varenne, A. Vessières, M. Salmain, P. Brossier, G. Jaouen, *J. Immunol. Methods* **1995**, *186*, 195 – 204.
[25] K. V. Kong, W. Chew, L. H. K. Lim, W. Y. Fan, W. K. Leong, *Bioconjugate Chem.* **2007**, *18*, 1370 – 1374.
[26] N. Metzler-Nolte, *Chimia* **2007**, *61*, 736 – 741.
[27] F. Noor, R. Kinscherf, G. Bonaterra, S. Walczak, S. Wölfl, N. Metzler-Nolte, *ChemBioChem* **2009**, *10*, 493 – 502.

